NASA Technical Memorandum 102295

Optimum Interface Properties for Metal Matrix Composites

Louis J. Ghosn
Sverdrup Technology, Inc.
NASA Lewis Research Center Group
Cleveland, Ohio

and

Bradley A. Lerch
National Aeronautics and Space Administration
Lewis Research Center
Cleveland, Ohio

August 1989

NASA

OPTIMUM INTERFACE PROPERTIES FOR METAL MATRIX COMPOSITES

Louis J. Ghosn
Sverdrup Technology, Inc.
NASA Lewis Research Center Group
Cleveland, Ohio 44135

and

Bradley A. Lerch
National Aeronautics and Space Administration
Lewis Research Center
Cleveland, Ohio 44135

SUMMARY

Due to the thermal expansion coefficient mismatch (CTE) between the fiber and the matrix, high residual stresses exist in metal matrix composite systems upon cool down from processing temperature to room temperature. An interface material can be placed between the fiber and the matrix to reduce the high tensile residual stresses in the matrix. A computer program was written to minimize the residual stress in the matrix subject to the interface material properties. The decision variables are the interface modulus, thickness and thermal expansion coefficient. The properties of the interface material are optimized such that the average distortion energy in the matrix and the interface is minimized. As a result, the only active variable is the thermal expansion coefficient. The optimum modulus of the interface is always the minimum allowable value and the interface thickness is always the maximum allowable value, independent of the fiber/matrix system. The optimum interface thermal expansion coefficient is always between the values of the fiber and the matrix. Using this analysis, a survey of materials was conducted for use as fiber coatings in some specific composite systems. The number of coating possibilities whose modulus and CTE fit the optimized values were limited. In order to increase the number of possible coating materials, elements with less than optimum modulus and CTE were examined. The residual stress state in the matrix and coating were calculated for these materials.

E-4964

INTRODUCTION

Metal matrix composites are presently being considered for aerospace applications due to their attractive high strength to low density ratio (ref. 1). The fiber system is usually a ceramic material with a high elastic modulus and low thermal expansion coefficient. The matrix system is an intermetallic with a low elastic modulus and high thermal expansion coefficient. During the manufacturing process of the composite, high complex residual stresses are introduced in each of the constituents (refs. 2 and 4) due to the thermal expansion mismatch. This has been found to cause cracking in some composites, especially those with brittle matrices (ref. 2). Using a simple two cylinder model to approximate the micromechanical behavior of a fiber/matrix system, Harris (ref. 3) has determined that the fiber is under a compressive state of stress, while the longitudinal and hoop stresses of the matrix are tensile and the radial stress is compressive. The tensile residual stresses are the cause of

the observed matrix cracking. Others have shown that the state of stress around the fiber is more complex making the radial stresses around the fiber oscillate between tension and compression depending on the fiber packing sequence (ref. 3). Although acknowledged, the effect of the neighboring fibers will not be considered in the present analysis.

The approach taken for the stress analysis in the present study is based on a three cylinder model (ref. 5), isolating one fiber with a layer of interface material and another layer of matrix material (fig. 1). The analysis considers only the residual stresses due to one cool down cycle. The analysis is limited to an elastic solution as a first approximation and it is assumed that each of the constituents are isotropic. For simplicity, the variation of material properties with temperature is not considered in the present study. In terms of the stress analysis, the longitudinal stresses are decoupled from the transverse stresses.

The objective of this paper is to define the properties of an interfacial layer necessary to minimize the local tensile residual stresses in the matrix thereby reducing the tendency towards cracking. This is accomplished by introducing an interfacial layer between the fiber and the matrix. The objective function of the minimization process is chosen to be the average distortion energy in the matrix and the interface. The decision variables are the elastic modulus, thermal expansion coefficient, and thickness of the interface layer. The distortional energy of the fiber is not included in the minimization function for the following two reasons: first, the fibers considered in this analysis are brittle ceramics, thus the distortional energy is not the corresponding failure criteria, and second the determined stresses in the fiber are compressive and the compressive strength of ceramics is very high.

STRESS ANALYSIS

The stress analysis is based on the self consistent method where a single fiber is assumed to be embedded in concentric cylinders of interface and matrix materials (fig. 1). The radii of the cylinders correspond to the volume fractions of each constituent in the original composite. In this analysis the longitudinal stresses are decoupled from the transverse stresses. The longitudinal stresses in each constituent, after a temperature drop of ΔT and assuming an isostrain in the z-direction, are given by:

$$\sigma_z^j = E_j \, (\alpha_\ell - \alpha_j) \, \Delta T \tag{1}$$

where E_j and α_j are the modulus and the thermal expansion coefficient respectively of constituent j (i.e., fiber (f), interface (i), and matrix (m)), ΔT is the change in temperature from processing to room temperature, α_ℓ is the effective longitudinal thermal expansion coefficient of the composite and can be approximated by:

$$\alpha_\ell = \left[\frac{v_f \alpha_f E_f + v_i \alpha_i E_i + v_m \alpha_m E_m}{v_f E_f + v_i E_i + v_m E_m} \right] \tag{2}$$

where the v_j's are the volume fraction of the constituents.

The transverse radial and hoop stresses are derived from the superposition of the thermal stresses and the confining pressures applied to each cylinder. The radial displacement (U_r) relations for each of the constituents are given by the free expansion, the poisson's effect of the longitudinal stresses and the confining pressure between two materials (ref. 6):

for the fiber

$$U_r^f = r\left\{\frac{(1 - \nu_f)}{E_f}(-p_i) + [\alpha_f - \nu_f(\alpha_\ell - \alpha_f)]\Delta T\right\} \tag{3}$$

for the interface

$$U_r^i = r\left\{\frac{(1 + \nu_i)}{E_i}\left[p_i \frac{\left(\frac{b}{r}\right)^2 + \frac{1 - \nu_i}{1 + \nu_i}}{\left(\frac{b}{a}\right)^2 - 1} - p_o \frac{\frac{1 - \nu_i}{1 + \nu_i} + \left(\frac{a}{r}\right)^2}{1 - \left(\frac{a}{b}\right)^2}\right] + [\alpha_i - \nu_i(\alpha_\ell - \alpha_i)]\Delta T\right\} \tag{4}$$

for the matrix

$$U_r^m = r\left\{\frac{(1 + \nu_m)}{E_m}\left[p_o \frac{\left(\frac{c}{r}\right)^2 + \frac{1 - \nu_m}{1 + \nu_m}}{\left(\frac{c}{b}\right)^2 - 1}\right] + [\alpha_m - \nu_m(\alpha_\ell - \alpha_m)]\Delta T\right\} \tag{5}$$

where r is the radial distance measured from the center of the fiber, and a, b and c are the radii of the fiber, the outer interface and the outer matrix, respectively, and p_i is the confining pressure between the fiber and the interface, and p_o is the confining pressure between the interface and the matrix, and ν_j is the poisson's ratio of constituent j.

The confining pressures can be determined in terms of the material properties and the dimensions of the constituents, by satisfying the continuity of the radial displacement at material boundaries, which are given by:

$$U_r^f|_a = U_r^i|_a \tag{6}$$

$$U_r^i|_b = U_r^m|_b \tag{7}$$

where $r = a$ is the fiber/interface boundary and $r = b$ is interface/matrix boundary.

Solving for the unknown pressures, a system of two simultaneous equations are derived and given by:

$$\begin{bmatrix} a_{11} & a_{12} \\ a_{21} & a_{22} \end{bmatrix} \begin{Bmatrix} p_i \\ p_o \end{Bmatrix} = \begin{Bmatrix} b_1 \\ b_2 \end{Bmatrix} \tag{8}$$

where:

$$a_{11} = -\frac{1-\nu_f}{E_f} - \left\{\frac{b^2+a^2}{b^2-a^2} + \nu_i\right\}\frac{1}{E_i}$$

$$a_{12} = \frac{2}{E_i\left(1-\frac{a^2}{b^2}\right)}$$

$$a_{21} = \frac{2}{E_i\left(\frac{b^2}{a^2}-1\right)}$$

$$a_{22} = -\frac{1}{E_i}\left\{\frac{b^2+a^2}{b^2-a^2} - \nu_i\right\} - \frac{1}{E_m}\left\{\frac{c^2+b^2}{c^2-b^2} + \nu_m\right\}$$

$$b_1 = \left\{(\alpha_i - \alpha_f) - \nu_i(\alpha_\ell - \alpha_i) + \nu_f(\alpha_\ell - \alpha_f)\right\}\Delta T$$

$$b_2 = \left\{(\alpha_m - \alpha_i) - \nu_m(\alpha_\ell - \alpha_m) + \nu_i(\alpha_\ell - \alpha_i)\right\}\Delta T$$

The residual radial and hoop stresses can now be solved for by using the elastic solution of thick cylinders under confining pressures (ref. 6). The stresses are given here for completeness in terms of the solution of equation 8:

for the fiber

$$\sigma_{rr}^f = \sigma_{\theta\theta}^f = -p_i \tag{9}$$

for the interface

$$\sigma_{rr}^i = -p_i\left[\frac{\left(\frac{b}{r}\right)^2-1}{\left(\frac{b}{a}\right)^2-1}\right] - p_o\left[\frac{1-\left(\frac{a}{r}\right)^2}{1-\left(\frac{a}{b}\right)^2}\right] \tag{10}$$

$$\sigma_{\theta\theta}^i = p_i\left[\frac{\left(\frac{b}{r}\right)^2+1}{\left(\frac{b}{a}\right)^2-1}\right] - p_o\left[\frac{1+\left(\frac{a}{r}\right)^2}{1-\left(\frac{a}{b}\right)^2}\right] \tag{11}$$

for the matrix

$$\sigma_{rr}^m = -p_o\left[\frac{\left(\frac{c}{r}\right)^2-1}{\left(\frac{c}{b}\right)^2-1}\right] \tag{12}$$

$$\sigma_{\theta\theta}^{m} = + p_o \left[\frac{\left(\frac{c}{r}\right)^2 + 1}{\left(\frac{c}{b}\right)^2 - 1} \right] \tag{13}$$

where σ_{rr} is the radial stress and $\sigma_{\theta\theta}$ is the tangential stress in a given constituent cylinder.

After cool down to room temperature, ΔT is defined as the difference between room and processing temperature and it will be negative. Given that p_i is positive, the radial and hoop stresses of the fiber are compressive and the longitudinal stresses are also compressive from equation 1 given that ΔT is negative and α_ℓ is greater than α_f. For the matrix, given that p_o is positive, the radial stress is compressive while the hoop stress is tensile. The longitudinal stress in the matrix is also tensile since α_ℓ is less than α_m. These tensile hoop and longitudinal stresses are the cause of radial and transverse matrix cracking observed in some composite systems.

MINIMIZATION FUNCTION

To minimize the local tensile stresses in the matrix, an interface layer is placed between the fiber and the matrix. The decision variables of the interface material are the modulus of elasticity E_i, the thermal expansion coefficient α_i, and the interface layer thickness t. The Poisson's ratio of the interface is assumed to be a constant value equal to 0.3. The objective function is assumed first to be the distortion energy in the matrix as governed by all the stress components of the matrix. The choice of the distortion energy as the minimization function is justified because of the matrix ductility and the restriction of the optimization to a single objective function. Therefore, the objective function can be written in terms of the stresses in the matrix as (ref. 6):

$$U_d = \int_V \frac{(1 + \nu)}{6E} \left\{ (\sigma_{rr} - \sigma_{\theta\theta})^2 + (\sigma_{\theta\theta} - \sigma_z)^2 + (\sigma_z - \sigma_{rr})^2 \right\} dV \tag{14}$$

Initial analysis has shown that by considering only the minimization of the matrix distortion energy, high relative stresses in the fiber and interface are observed. The resulting high compressive stresses in the fiber could be tolerated if the fiber system is a brittle ceramic with very high compressive strength. On the other hand, the high tensile hoop stress in the interface cannot be tolerated. Therefore, the objective function was modified to include the distortion energy of the interface. The final objective function used to minimize the residual stresses in the matrix was taken to be the distortion energy in the matrix plus the distortion energy in the interface divided by the total volume of the matrix and interface:

Objective function

$$\underset{\text{minimize}}{f(E_i,\ \alpha_i,\ t)} = \frac{\int_V U_d(\text{matrix})\ dV + \int_V U_d(\text{interface})\ dV}{\text{volume matrix} + \text{volume interface}} \tag{15}$$

subject to:

$$E_{Lb} \leq E_i \leq E_{ub}$$

$$\alpha_{Lb} < \alpha_i < \alpha_{ub}$$

$$t_{Lb} \leq t \leq t_{ub}$$

where superscripts ub and Lb stand for the upper and lower bound, respectively. The constraints on the decision variables are required to guarantee a realistic solution which must fall into the range of typical material properties. The range of the interface modulus is assumed to be between 69 and 517 GPa. The lower and upper bound of the interface thermal expansion coefficient is 4×10^{-6} 1/°C and 20×10^{-6} 1/°C, respectively. The thickness, t has zero as a lower bound and an arbitrary upper bound as will be seen next in the application section.

APPLICATIONS AND RESULTS

A computer program was written to minimize the average distortion energy in the matrix and the interface. The minimization routine (from the IMSL library) (ref. 7) uses the Quasi-Newton iteration method from given starting points. Twenty different initial sets of points are used to guarantee convergence to a global minimum. The first run consisted of a single fiber system and a variance of matrix properties with a temperature drop of -800 °C. The upper and lower bound of the interface modulus is taken to be 69 and 517 GPa, respectively, corresponding to the modulus of materials ranging from aluminum to carbon. The minimization shows that the optimum elastic modulus is controlled by the lower bound, taken to be 69 GPa (10 Msi). The optimum interface thickness always reaches the upper bound at the global minimum. Therefore, two different upper bound thicknesses are considered. In case 1 the ratio (t/d) of the upper bound thickness to the fiber diameter is 0.12 and for case 2, t/d = 0.20. For a fiber diameter of 145 μm (typical of the majority of fibers used in today's MMC's), this translates to interface thicknesses of 17.4 and 29 μm, typical of standard coating thicknesses. Figures 2 and 3 show the variation of the optimum interface thermal expansion coefficient as a function of the matrix material properties for t/d = 0.12 and t/d = 0.20, respectively. The selected fiber is SiC, the most common reinforcement fiber for today's MMC's, having an elastic modulus E_f = 427.5 GPa and a thermal expansion coefficient $\alpha_f = 4.9\times10^{-6}$ 1/°C. The initial fiber volume fraction is 0.4. For this analysis, the matrix volume fraction is kept constant at 0.6. The optimum interface thermal expansion coefficient increases with increasing matrix modulus and matrix thermal expansion coefficient. A greater interface thickness also results in an increase of the optimum interface thermal expansion coefficient. The effect of the interface layer on the distortion energy (i.e., the objective function) is considered by comparing figures 4 to 6

for different matrix thermal expansion coefficients. The reduction in the distortion energy relative to a composite without an interface is in the range of 30 to 40 percent with $t/d = 0.12$, and for $t/d = 0.20$ this reduction range is 44 to 72 percent. The specific value of the reduction for a given t/d depends on the matrix material properties. The effect of the interface layer on the actual stress components is limited to only a set of candidate composite systems as seen next.

The remainder of this study dealt with finding the optimum interface layer properties for some candidate matrix (Ti-15-3, Ti_3Al, NiAl) and fiber (SiC, TiB_2) systems. Table I summarizes the assumed material properties of the two fiber systems (SiC and TiB_2) and the three metal matrix systems(Ti-15-3, Ti_3Al and NiAl) used. In table I, E is the room temperature elastic modulus. The thermal expansion coefficient was approximated by taking the slope of the experimental strain versus temperature curve using the end points. The temperature change assumed was -800 °C which is the difference between room temperature and half the melting temperature of the various matrix materials. The selection of half the melting temperature as the upper limit is prompted from the assumption that above one half the melting temperature the residual stresses will be relieved due to creep or annealing (ref. 8). The optimum thermal expansion coefficients of the interface layer for the above composite systems are shown in table II for two interface thicknesses. When the modulus of elasticity of the matrix is close to the optimum interface modulus (69 GPa) (e.g., Ti-15-3 or Ti_3Al), the interface thermal expansion coefficient can be approximated as the average of the thermal coefficients of the matrix and the fiber. When the modulus of elasticity of the matrix is higher than the interface (e.g., for NiAl), the optimum thermal expansion coefficient of the interface tends toward the matrix value.

The effect of the optimum interface on the maximum stresses in the matrix are shown in table III for $r = b$. The percent drop of the stress in the matrix is generally largest for the NiAl matrix system and smallest for Ti_3Al. To combine all the stress components, the maximum effective stress in the matrix based on the Von-Mises (distortion energy) criterion is shown in table 4 with and without the interface. The effective stress in the matrix decreases as the interface thickness (t/d) increases. For the NiAl matrix system, the effective stress is decreased well below the yield stress of the material when an interface layer with thickness $t/d = 0.2$ is introduced, thus indicating the benefit of this coating. Also, it should be emphasized that TiB_2 offers a large reduction in residual stresses compared to SiC (tables III and IV) for all of the matrix materials investigated. For the Ti_3Al matrix, this reduction is sufficient to reduce the effective stress of the matrix below the yield point. The effective stresses in the interface are also shown in table V for comparison at two locations: at $r = a$ and $r = b$. Contrary to what is suggested in reference 9, the state of stress in the interface is not under hydrostatic compression since the effective stress based on the Von-Mises criterion is not zero. Although the optimized interface decreases the effective stresses in the matrix, the compressive stresses in the fiber are increased with increasing interface thickness. However, the maximum compressive stress calculated after optimization was still below the fiber compressive strength for all the composite systems analyzed.

The variation of the effective longitudinal and transverse moduli of the composite is shown in table VI. The effective moduli of the composite are

determined from a one-dimensional theory of elasticity with constant displacement and constant force for the longitudinal and transverse modulus respectively. The effect of the low modulus interface layer is to decrease the effective modulus of the composite as seen in table VI. Therefore, an optimally designed interface layer can reduce the deleterious tensile residual stresses in the matrix of a metal matrix composite system. The main motivation for reducing the residual stresses in the matrix is to avoid matrix cracking upon cool-down from processing temperature to room temperature therefore reducing the number of initial flaws which in turn should increase the fatigue life of the metal matrix composites. In practice, the choice of an appropriate coating material is difficult due to the limited number of possibilities as is described below.

A variety of elements and compounds were surveyed for use as possible coating materials. These materials are listed in table VII, together with their CTE, and modulus. Since exposure to high temperatures and weight reduction are important factors in choosing high temperature materials, the melting temperatures and density have also been included in table VII for completeness. The desired coating properties for any of the composite systems required a low modulus (~69 GPa) and a CTE as listed in table II. Only the thicker coating (i.e., t/d = 0.20) is considered in the remaining discussion. For use with the three matrix materials and the two fibers, only six possible materials from table VII had elastic moduli ~69 GPa (i.e., actual range of 57 to 80 GPa) and these are given in table VIII. Since the number is small, the first group of coating materials in table VIII also includes those materials with moduli up to 103 GPa, which doubles the possible number of coating materials. Based on their CTE, the possible coating systems were chosen from this table for each composite system. Those materials indicated with a "x" are the best choices for use as a coating, those marked with a dash are less than optimum possibilities, but may still be usable. The criteria for determining best choices or less than optimum choices are as follows:

(1) Only materials having moduli $\leq$103 GPa can qualify as best choices. Materials having larger moduli were classified as less than optimum.

(2) Best choices had CTE values within $\pm 2 \times 10^{-6}$ 1/°C of the optimized values.

(3) Less than optimum choices had CTE values at the optimized CTE value $\pm 3 \times 10^{-6}$ 1/°C.

Based on these selection criteria, the following two points were observed:

(1) The best candidates for coatings are generally metals. Ceramics/intermetallics are not appropriate as coating materials due to their extremely high moduli. Silicon Nitride and Ti_3Al are exceptions.

(2) There are a limited number of coating possibilities which satisfy the modulus and CTE requirements.

To increase the number of possible coating candidates, materials having moduli between 103 and 207 GPa are also given in table VIII. These materials were again selected based on the proximity of their CTE to the optimum value given in table II. Note that these are less than optimum choices since their

moduli are higher. Analysis has shown (table IX) that the optimum CTE for coating materials with moduli of 138 and 207 GPa does not vary much from that of materials with a modulus of 69 GPa (compare table IX with table II). However, there is an increase in the matrix stress, as observed in table X, when using coatings with a higher than optimum modulus. The increase appears to be minimal for the Ti-15-3 and Ti_3Al matrix systems, but is significant for the NiAl system: a manifestation of the higher modulus and CTE of NiAl.

The ultimate selection of the fiber coating will also depend on its chemical compatibility with both the fiber and the matrix. The small choice of coating materials listed in table VII will be reduced to an even smaller number when chemical compatibility is taken into account. Therefore, to increase the possible number of coatings, nonoptimized materials were also examined for use in the SiC/NiAl composite, since this composite shows the largest benefit from the use of a compliant coating. A variety of coating elements are given in table XI along with the effective stress in the matrix and the interface. The optimum coating for the SiC/NiAl system is Au, yielding the lowest effective stresses in both the matrix and the coating. Other coatings (e.g., Cu, Co) will reduce the matrix effective stress to a lower value than the stress which is obtained when an optimized modulus and CTE for the interface are used, but have the disadvantage that the coating stress will greatly increase. The high effective stress in the coating could lead to fiber/matrix debonding, although the actual effects of such a high stress in the coating are unknown.

Experimental work is needed to determine in which constituents the stresses should be kept minimal. Table XI also indicates that the optimum coating materials are not intuitively obvious based solely on having a CTE between that of the fiber and the matrix. For example, Pt has a CTE halfway between that of the fiber and the matrix, yet yields very high effective stresses in the matrix. This indicates the important relationship between the modulus and the CTE.

CONCLUSIONS

An analysis was performed to determine the optimum interface material properties required to reduce the tensile residual stresses in a given metal matrix composite system. The objective was to study the concept of a compliant layer to minimize the tensile residual stresses in the matrix upon cool down from processing to room temperature. Based on the elastic isotropic analysis of a three cylinder model with constituent properties assumed to be temperature independent and the longitudinal stresses decoupled from the transverse stresses, the following points were concluded:

1. A well designed interface layer can reduce the tensile residual stresses in a metal matrix composite system.

2. To reduce the residual stresses in the matrix, the average distortion energy in the matrix and the interface was minimized.

3. The optimum interface thickness was always at the given upper bound for this particular objective function.

4. The optimum interface modulus was always at the lower bound for this particular objective function.

5. For a given fiber system, the optimum interface thermal expansion coefficient increases with increasing matrix modulus and thermal expansion coefficient.

6. For low matrix elastic modulus the optimum thermal expansion coefficient can be approximated by the average thermal expansion coefficient of the matrix and fiber.

7. For high matrix modulus, the optimum thermal expansion coefficient of the interface approaches the matrix value.

8. The effect of the low modulus optimum interface is to decrease the effective modulus of the composite.

9. From a variety of materials, coating selections were made to reduce the residual stresses in the matrix and coating for composites containing the fiber constituents TiB_2 and SiC and matrix constituents Ti-15-3, Ti_3Al and NiAl.

10. Selection of TiB_2 fibers over SiC fibers results in significantly lower effective stresses in the matrix for all the matrix materials studied herein.

REFERENCES

1. Stephens, J.R.; and Nathal, M.V.: Status and Prognosis for Alternative Engine Materials. Superalloys 1988, D.N. Duhl, et al., eds., Metallurgical Society of AIME, 1988, pp. 183-192.

2. Chou, T.W.; Kelly, A.; and Okura, A.: Fibre-Reinforced Metal-Matrix Composites. Composites, vol. 16, no. 3, July 1985, pp. 187-206.

3. Harris, B.: Shrinkage Stresses in Glass/Resin Composites. J. Mater. Sci., vol. 13, no. 1., Jan. 1978, pp. 173-177.

4. Haener, J., et al.: Investigation of Micromechanical Behavior of Fiber Reinforced Plastics. USAAV LABS-TR-67-66, (Avail. NTIS, 1968 AD-667901).

5. Vedula, M.; Pangborn, R.N.; and Queeney, R.A.: Modification of Residual Thermal Stress in a Metal-Matrix Composite with the use of a Tailored Interfacial Region, Composites, vol. 19, no. 2, Mar. 1988, pp. 133-137.

6. Saada, A.S.: Elasticity Theory and Applications. Robert Krieger Publisher, 1983.

7. IMSL Math/Library User's Manual Version 1., International Mathematical and Statistical Libraries Inc. Apr. 1987.

8. Dieter, G.E.: Mechanical Metallurgy, 2nd ed., McGraw-Hill, 1976, pp. 451-489.

9. Nimmer, R.P.; and Banket, R.J.: Micromechanical Modeling of Fiber/Matrix Interface Effects in SiC/Ti MMC. Presented at 13th Annual Conference on Composites Materials and Structures, Cocoa Beach, FL, Jan. 1989 (to be published in Ceram. Eng. Sci. Proc.).

10. Metallic Materials and Elements for Aerospace Vehicle Structures. MIL-HDBK-5E, June 1987, pp. 5-121 to 5-125.

11. Lerch, B.A.: Ongoing Research. NASA Lewis Research Center, Cleveland, OH.

12. Textron Specialty Materials Data Sheet, Silicon Carbide Composite Materials.

13. Brindley, P.K.: Ongoing Research NASA Lewis Research Center, Cleveland, OH.

14. Desai, P.D.; and Chaney, J.F.: Thermal Linear Expansion of TiB_2. High Temperature Materials - Mechanical, Electronic and Thermophysical Properties Information Analysis Center, Purdue University, 1988.

15. McDanels, D.L., and Stephens, J.R.: High Temperature Engine Materials Technology - Intermetallic and Metal Matrix Composites. NASA TM-100844, 1988.

16. Harmouche, M.R.; and Wolfenden, A: Temperature and Composition Dependence of Young's Modulus in Polycrystalline B2 Ni-Al. J. Test Eval., vol. 15, 1987, pp. 101-104.

17. Clark, R.W.; and Whittenberger, J.D.: Thermal Expansion of Binary CoAl, FeAl, and NiAl Alloys. Thermal Expansion 8, T.A. Hahn, ed., Plenum Press, 1984, pp. 189-196.

18. Shaffer, P.T.B.: Materials Index, (Handbooks of High - Temperature Materials, No. 1) Plenum Press, 1964.

19. Metals Handbook, Vol. 1, Properties and Selection of Metals, 8th ed., ASM, Metals Park, OH, 1961.

20. Barrett, C.R; Nix, W.D.; and Tetelman, A.S: The Principles of Engineering Material. Prentice-Hall Inc., 1973.

TABLE I. - ASSUMED CONSTITUENT PROPERTIES

[Numbers in parentheses indicate references.]

Fiber	SiC[12]	TiB_2
E, GPa	427.5	365.4[15]
α, 1/°C	4.9×10^{-6}	8.0×10^{-6}[14]

Matrix	Ti-15-3	Ti_3Al[13]	NiAl
E, GPa	100.0[11]	75.2	237.2[16]
σ_{yield}, MPa	834.3[11]	379.2	1765.1
σ, 1/°C	8.5×10^{-6}[10]	11.7×10^{-6}	15.6×10^{-6}[17]

TABLE II. - OPTIMUM THERMAL EXPANSION COEFFICIENT OF THE INTERFACE AFTER MINIMIZATION

Composite system		t/d	
		0.12	0.20
Matrix	Fiber	α_i, 1/°C	
Ti-15-3	SiC	6.8×10^{-6}	7.1×10^{-6}
	TiB_2	8.3	8.3
Ti_3Al	SiC	7.9×10^{-6}	8.4×10^{-6}
	T_iB_2	9.7	10.0
NiAl	SiC	14.1×10^{-6}	14.6×10^{-6}
	TiB_2	14.7	15.0

TABLE III. - MAXIMUM MATRIX STRESSES AT THE INNER RADIUS (r = b) in MPa

[Numbers in parentheses indicate percent drop as compared to no interface.]

	t/d	Matrix					
		Ti-15-3		Ti_3Al		NiAl	
		Fiber					
		SiC	TiB_2	SiC	TiB_2	SiC	TiB_2
σ_z (longi-tudinal)	0.00	213(--)	28(--)	324(--)	170(--)	1108(--)	731(--)
	.12	184(14)	24(14)	287(11)	149(12)	868(22)	562(23)
	.20	166(22)	21(25)	263(19)	135(21)	739(33)	474(35)
$\sigma_{\theta\theta}$ (tangen-tial)	0.00	324(--)	69(--)	461(--)	242(--)	2055(--)	1392(--)
	.12	242(25)	33(52)	367(20)	196(19)	1277(38)	883(37)
	.20	207(36)	28(59)	322(30)	171(29)	987(52)	681(51)
σ_{rr} (radial)	0.00	-140(--)	-30(--)	-198(--)	-103(--)	-881(--)	-596(--)
	.12	-104(26)	-14(53)	-157(21)	-84(18)	-547(38)	-378(37)
	.20	-89(36)	-12(60)	-138(30)	-73(29)	-423(52)	-292(51)

TABLE IV. - MAXIMUM EFFECTIVE STRESS (at r = b) IN THE MATRIX (IN MPa) BASED ON THE VON-MISES CRITERION

[Numbers in parenthesis indicate percent drop as compared to no interface.]

Composite system		t/d			σ_{yield}, MPa
Matrix	Fiber	0.0	0.12	0.20	
Ti-15-3	SiC TiB_2	422 86	321(24) 43(50)	277(34) 37(57)	834 834
Ti_3Al	SiC TiB_2	602 315	490(19) 260(17)	434(28) 229(27)	379 379
NiAl	SiC TiB_2	2595 1754	1655(36) 1135(35)	1304(50) 888(49)	1766 1766

TABLE V. - EFFECTIVE STRESS (IN MPa) AT TWO LOCATIONS IN THE INTERFACE (AT THE FIBER/COATING INTERFACE, r = a AND AT THE COATING/MATRIX INTERFACE, r = b) BASED ON THE VON-MISES CRITERION

Composite system		t/d			
		0.12		0.20	
Matrix	Fiber	r = a	r = b	r = a	r = b
Ti-15-3	SiC TiB_2	199 28	139 19	215 30	123 17
Ti_3Al	SiC TiB_2	306 169	214 117	340 188	194 105
NiAl	SiC TiB_2	995 695	705 489	979 684	566 391

TABLE VI. - EFFECTIVE ELASTIC LONGITUDINAL AND TRANSVERSE MODULI IN GPa IN THE COMPOSITE WITH AND WITHOUT INTERFACE

[Numbers in parenthesis indicate percent drop as compared to no interface.]

Composite system		t/d					
		0.00		0.12		0.20	
Matrix	Fiber	EL	ET	EL	ET	EL	ET
Ti-15-3	SiC TiB_2	231 206	144 141	181(22) 165(20)	116(19) 114(19)	161(30) 148(28)	107(26) 106(25)
Ti_3Al	SiC TiB_2	216 191	112 110	166(23) 150(21)	94(16) 93(15)	146(32) 133(30)	89(21) 88(20)
NiAl	SiC TiB_2	313 289	289 276	263(16) 247(15)	194(33) 190(31)	243(22) 230(20)	171(41) 169(39)

TABLE VII. - SURVEY OF CANDIDATE COATING MATERIALS
(REFS. 18, 19, AND 20)

	Density, g/cm^3	CTE, $1/°C$	Melting temperature, °C	E, GPa
Elements				
Al	2.7	23.9×10^{-6}	660	62
Ag	10.5	25.9	961	71
Au	19.3	17.0	1063	80
Be	1.8	18.0	1300	276
Graphite	1.9	5.0	----	7
Co	8.9	18.5	1490	207
Cr	7.1	11.0	1890	248
Cu	8.9	21.5	1083	117
Dy	8.5	12.3	1407	63
Fe	7.9	12.0	1535	200
Gd	7.9	10.0	1312	57
Hf	12.1	6.0	2200	138
Ir	22.4	7.9	2400	524
Mn	7.2	50.7	1260	159
Mo	10.2	5.8	2620	317
Nb	8.6	8.0	2410	103
Nd	6.9	9.0	840	38
Ni	9.2	17.1	1455	221
Os	22.4	5.6	2700	558
Pd	12.0	14.0	1555	112
Pt	21.4	10.5	1780	147
Re	21.0	6.9	3130	460
Rh	12.5	10.8	1965	241
Si	2.3	4.0	1430	110
Ta	16.8	7.1	3000	186
Ti	4.5	10.6	1750	107
V	6.0	10.7	1735	124
W	19.3	4.8	3400	407
Zr	6.4	5.3	1830	94
Carbides				
Al_4C_3	3.0	---------	2800	-----
B_4C	2.5	5.5×10^{-6}	>3500	448
Cr_3C_2	6.7	10.0	1850	-----
HfC	12.7	6.3	3887	425
NbC	7.8	7.1	3500	339
SiC	3.2	5.1	2500	401
TiC	4.9	8.8	3160	439
WC	15.7	4.9	2870	668
Nitrides				
AlN	3.3	5.6×10^{-6}	2230	345
BN*	2.3	0.8/7.5	2730	86/34
Si_3N_4	3.5	2.9	1900	90
TiN	5.2	9.4	2945	250
Oxides				
Al_2O_3	4.0	8.5×10^{-6}	2015	345
BeO	3.0	9.0	2520	314
Fe_2O_3	5.1	12.3	1455	-----
MgO	3.6	13.6	2800	250
TiO_2	----	8.8	1920	-----
$MoSi_2$	6.2	8.5	2030	276
Compounds				
NiAl	5.9	15.6×10^{-6}	1638	237
FeAl	6.1	21.8	1340	246
Ti_3Al	5.1	11.7	1500	75

*Anisotropic.

TABLE VIII. - SELECTED INTERFACE COATINGS

[x indicates best coating materials; - indicates possible coating materials.]

	E_i, GPa	CTE_i, 1/°C	Ti-15-3		Ti_3Al		NiAl	
			SiC	TiB_2	SiC	TiB_2	SiC	TiB_2
$E_i \leq 103$ GPa								
C	7	5×10^{-6}	x	-	-			
Gd	57	10	-	x	x	x		
Al	62	24						
Dy	63	12				x	-	-
Ag	71	26						
Ti_3Al	75	12					-	-
Au	80	17					x	x
Si_3N_4	90	3						
Zr	94	5	x	-	-			
Nb	103	8	x	x	x	x		
$103 < E_i \leq 138$								
Ti	107	11×10^{-6}		-	-	-		
Si	110	4	-					
Pd	112	14					-	-
Cu	117	22						
V	124	11		-	-	-		
Hf	138	6	-	-	-			
$138 < E_i \leq 207$								
Pt	147	11×10^{-6}		-	-	-		
Mn	159	51						
Ta	186	7	-	-	-	-		
Fe	200	12				-	-	-
Co	207	19						

TABLE IX. - OPTIMUM INTERFACE CTE FOR INTERFACE MATERIALS HAVING MODULI > 103 GPa

Matrix	Fiber	t/d	
		0.12	0.20
		CTE_i, 1/°C	
E_i = 138 GPa			
Ti-15-3	SiC	6.5×10^{-6}	6.8×10^{-6}
	TiB_2	7.0	7.2
Ti_3Al	SiC	7.4	7.9
	TiB_2	8.1	8.5
NiAl	SiC	12.5	13.1
	TiB_2	13.0	13.5
E_i = 207 GPa			
Ti-15-3	SiC	6.4×10^{-6}	6.6×10^{-6}
	TiB_2	6.9	7.1
Ti_3Al	SiC	7.2	7.7
	TiB_2	7.9	8.3
NiAl	SiC	11.9	12.5
	TiB_2	12.5	13.0

TABLE X. - MAXIMUM MATRIX STRESSES (IN MPa) AT THE INNER RADIUS (r = b) AS A FUNCTION OF INTERFACE MODULUS; t/d = 0.20

[Numbers in parentheses indicate percent drop as compared to no interface.]

	E_i, GPa	Matrix					
		Ti-15-3		Ti_3Al		NiAl	
		Fiber					
		SiC	TiB_2	SiC	TiB_2	SiC	TiB_2
σ_z (longitudinal)	69	166(22)	21(25)	263(19)	135(21)	739(33)	474(35)
	138	166(22)	22(21)	263(19)	135(21)	740(33)	475(35)
	207	166(22)	22(21)	263(19)	135(21)	743(33)	478(35)
$\sigma_{\theta\theta}$ (tangential)	69	207(36)	28(59)	322(30)	171(29)	987(52)	681(51)
	138	228(30)	31(55)	348(25)	185(24)	1199(42)	823(41)
	207	236(27)	32(54)	357(23)	189(22)	1280(38)	875(37)
σ_{rr} (radial)	69	-89(36)	-12(60)	-138(30)	-73(29)	-423(52)	-292(51)
	138	-98(30)	-13(57)	-149(25)	-79(23)	-514(42)	-353(41)
	207	-101(28)	-14(53)	-153(23)	-81(21)	-549(38)	-375(37)

TABLE XI. - EFFECTIVE STRESS (IN MPa) IN THE MATRIX AND INTERFACE FOR VARIOUS COATING MATERIALS IN THE SiC/NiAl COMPOSITE SYSTEM

Element	E_i, GPa	CTE_i, 1/°C	σ_{eff}, matrix (r = b)	σ_{eff}, interface (r = a)
Gd	57	10.0×10^{-6}	1554	662
Dy	63	12.3	1438	811
Au	80	17.0	1163	1245
Nb	103	8.0	1904	664
Pd	112	14.0	1435	1294
Cu	117	21.5	850	2139
Pt	147	10.5	1776	1067
Ta	186	7.1	2138	662
Fe	200	12.0	1678	1545
Co	207	18.0	1052	2854

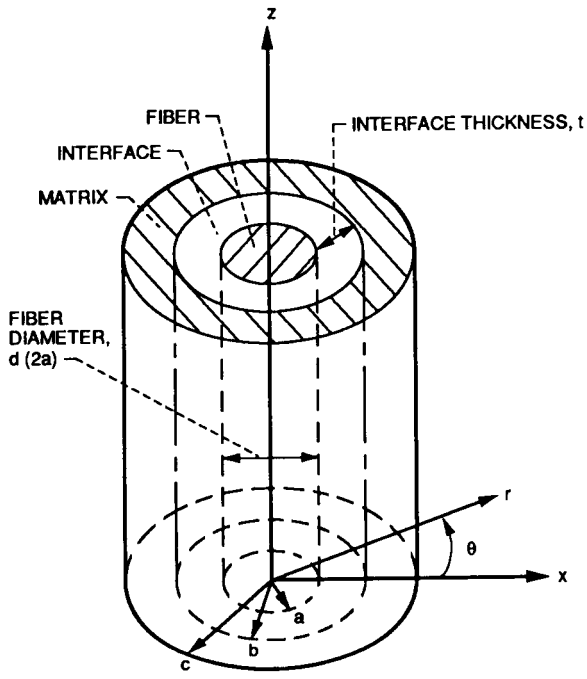

Figure 1. - Three cylinder model.

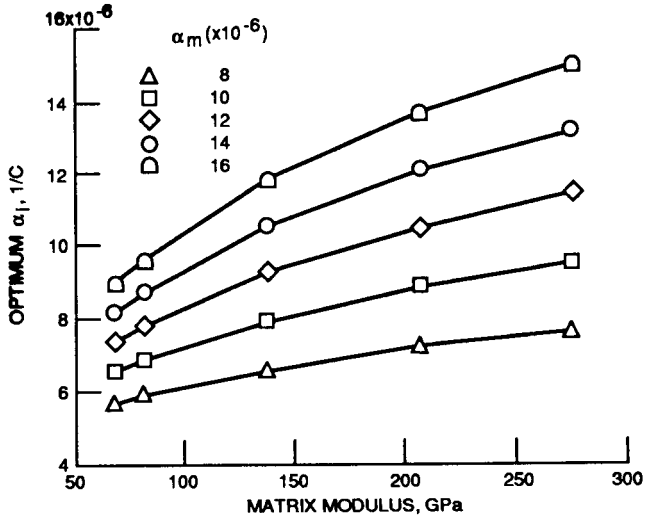

Figure 2. - Optimum interface thermal expansion coefficient as a function of matrix properties, for t/d = 0.12, and for a SiC fiber system.

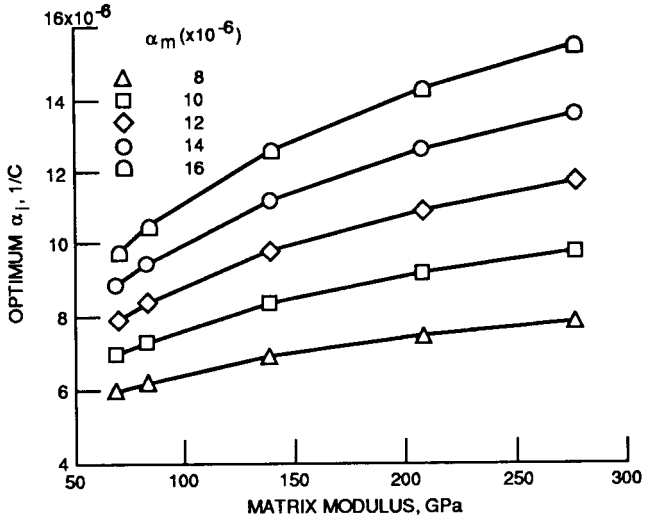

Figure 3. - Optimum interface thermal expansion coefficient as a function of matrix properties, for t/d = 0.20, and for a SiC fiber system.

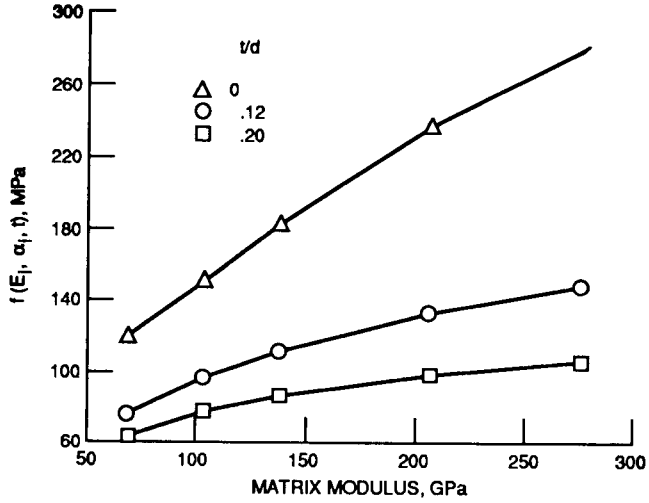

Figure 4. - Average distortion energy as a function of matrix modulus and interface thickness, for $\alpha_m = 8 \times 10^{-6}$ 1/C, and a SiC fiber system.

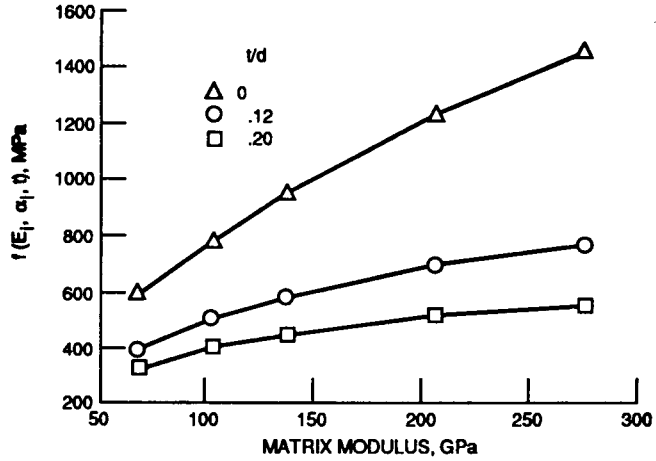

Figure 5. - Average distortion energy as a function of matrix modulus and interface thickness, for $\alpha_m = 12 \times 10^{-6}$ 1/C, and a SiC fiber system.

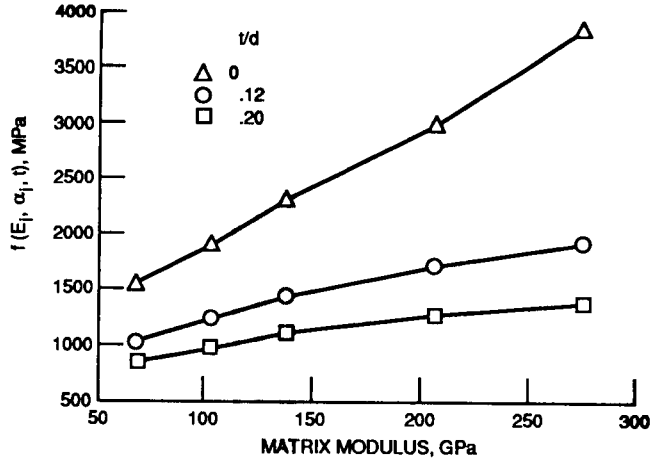

Figure 6. - Average distortion energy as a function of matrix modulus and interface thickness, for $\alpha_m = 16 \times 10^{-6}$ 1/C, and a SiC fiber system.

NASA
National Aeronautics and Space Administration

Report Documentation Page

1. Report No.	2. Government Accession No.	3. Recipient's Catalog No.
NASA TM-102295		

4. Title and Subtitle	5. Report Date
Optimum Interface Properties for Metal Matrix Composites	August 1989
	6. Performing Organization Code

7. Author(s)	8. Performing Organization Report No.
Louis J. Ghosn and Bradley A. Lerch	E-4964
	10. Work Unit No. 510-01-0A

9. Performing Organization Name and Address	11. Contract or Grant No.
National Aeronautics and Space Administration Lewis Research Center Cleveland, Ohio 44135-3191	
	13. Type of Report and Period Covered Technical Memorandum

12. Sponsoring Agency Name and Address	14. Sponsoring Agency Code
National Aeronautics and Space Administration Washington, D.C. 20546-0001	

15. Supplementary Notes

Louis J. Ghosn, Sverdrup Technology, Inc., NASA Lewis Research Center Group, Cleveland, Ohio 44135; Bradley A. Lerch, NASA Lewis Research Center.

16. Abstract

Due to the thermal expansion coefficient mismatch (CTE) between the fiber and the matrix, high residual stresses exist in metal matrix composite systems upon cool down from processing temperature to room temperature. An interface material can be placed between the fiber and the matrix to reduce the high tensile residual stresses in the matrix. A computer program was written to minimize the residual stress in the matrix subject to the interface material properties. The decision variables are the interface modulus, thickness and thermal expansion coefficient. The properties of the interface material are optimized such that the average distortion energy in the matrix and the interface is minimized. As a result, the only active variable is the thermal expansion coefficient. The optimum modulus of the interface is always the minimum allowable value and the interface thickness is always the maximum allowable value, independent of the fiber/matrix system. The optimum interface thermal expansion coefficient is always between the values of the fiber and the matrix. Using this analysis, a survey of materials was conducted for use as fiber coatings in some specific composite systems. The number of coating possibilities whose modulus and CTE fit the optimized values were limited. In order to increase the number of possible coating materials, elements with less than optimum modulus and CTE were examined. The residual stress state in the matrix and coating were calculated for these materials.

17. Key Words (Suggested by Author(s))	18. Distribution Statement
Composites; Metal matrix; Thermal residual stresses; Cylindrical model; Interface properties	Unclassified – Unlimited Subject Category 39

19. Security Classif. (of this report)	20. Security Classif. (of this page)	21. No of pages	22. Price*
Unclassified	Unclassified	20	A03

*For sale by the National Technical Information Service, Springfield, Virginia 22161